Multi-objective analysis of an influence of a brine mineralization on an optimal evaporation temperature in ORC power plant

Marcin Jankowski[1,*], *Sławomir* Wiśniewski[1], and *Aleksandra* Borsukiewicz[1]

[1]West Pomeranian University of Technology, Chair of Thermal Engineering, Al. Piastów 19, 70-310, Szczecin, Poland

Abstract. The fact that Organic Rankine cycle system is very promising technology in terms of electricity production using low grade heat sources, necessitates constant research in order to determine the best cycle configuration or choose the most suitable working fluid for certain application. In this paper, multi-objective optimization (MOO) approach has been applied in order to conduct an analysis that is to resolve if there is an influence of a mineralization of a geothermal water on an optimal evaporation temperature in ORC power plant with R1234yf as the working fluid.

1 Introduction

Organic Rankine Cycle system (ORC) is constantly developing technology in past several decades. The main advantage of such systems is the availability of effective conversion low grade heat into power. Moreover, they are characterised by simple construction, low negative environmental influence and relatively high effectiveness. In view of the above advantages, a lot of research is still being conducted in order to ensure the most efficient work of designed ORC system. These studies are taking into account different technical and ecomomic performance indicators, called objective functions, which are to be minimized or maximized. Discussed criteria include: energy efficiency η_I (first law efficiency), exergy efficiency η_{II} (second law efficiency), net power output W_{net}, heat transfer area A, overall heat transfer coefficient k, overall cost of the system C, total exergy destruction rate δB_{tot} [1] or size parameter SP, which allows to initially evaluate the size of a turbine [2]. Some authors also used different combinations of these quantities. Shengjun et. al [3] concucted thermo-economic optimization of subcritical ORC and transcritical power cycle system for low temperature geothermal power generation using several objective functions: ratio of heat transfer area and net power output, also known as APR parameter, or levelized energy cost LEC. Roy et. al [4] carried out performance analysis of an ORC with superheating under different heat source temperature conditions using so called availability ratio Φ, which is defined as the ratio of the available energy (difference between heat obtained from the thermal source and total exergy destruction in the system) to the total energy obtained from the thermal source. Guo et. al [5] conducted thermodynamic analysis of waste heat power generation system. One of the applied objective function was so called sustainability index SI, which is also used in this paper.

Most of the conducted studies converge single-objective analysis, which are focused on optimizing one of the above performance indicators. Much less attention has been paid to multi-objective optimization (MOO). This approach allows to carry out more comprehensive analysis, using more than one objective function, which means that ORC system can be optimized from both thermodynamic and ecomonic perspectives. Moreover, the selection process of the working fluid can be also optimised including several criteria [6].

Wang et. al [7] carried out multi-objective optimization of an ORC for low grade waste heat recovery using evolutionary algorithm. The authors used exergy efficiency and capital cost as performance indicators of the system. Xiao et. al [8] conducted multi-objective optimization of evaporation and condensation temperatures for subcritical ORC, using sustainability index SI and the ratio of the cost of the system C to net power output as objective functions. The authors solved optimization problem using linear weighted evaluation function. Toffolo et. al [9] made the optimal selection of working fluid and design parameters in ORC system, using multi-criteria approach. The objective functions that the authors applied, was levelized cost of electricity $LCOE$, which considers the annual energy production of the system or specific investment cost SIC defined as the ratio between total investment cost and net power output.

In several cases, it is very important to not only seeking to improve all thermodynamic and economic indexes, but also include some inconveniences of the system. Therefore, in case of geothermal water, which is the energy source in the system analysed in this paper, the level of mineralization M of a brine should be considered. In order to solve this problem, multi-objective optimization has been carried out using weighted sum method [10] with global function G, which is to be minimized.

* Corresponding author: marcin.jankowski@zut.edu.pl

2 Calculation model of a system

2.1 System description

The energy source of the system has a significant impact on the overall performance and effectiveness of ORC power plant and it is important to carry out complex analysis in order to determine the optimal working parameters of the ORC. In case of considered system, geothermal water (brine) has been used to supply ORC power plant. One of the crucial property of such fluid is mineralization *M*. It is worth to emphasise that this parameter can quite considerably vary depending on local hydrogeothermal conditions. The level of salinity of the brine affects its values of basic thermophysical properties, such as: specific heat c_{p1} and density ρ_1, so in calculation procedure, these parameters should be considered as function of either temperature and mineralization.

The ORC system, as shown in figure 1 and 2, works as classical power plant. Slightly superheated (point 1) vapour flows into the expander and its enthalpy is converted to useful work of the turbine. The low pressure vapour (point 2) is cooled (to the state corresponding to point 2") and phase change occurs in condenser (cold water is a coolant). Then the saturated liquid (3) is pumped to higher pressure and goes to the inlet of vapour generator, where it is heated up, evaporated and, optionally, superheated.

The choice of the working fluid affects substantially the overall performance of ORCs and a lot of analysis have been done in order to choose the best one for certain configuration of the system [11], [12], [13]. In this paper, R1234yf has been chosen as one of the most promising working fluid, because of its beneficial impact on an effectiveness of ORC, as well for a favourable environmental indicators, such as: *ODP=0* and *GWP=4* [14].

As more attention in calculation procedure has been devoted to the evaporation process of the working fluid, in figure 3 only vapour generator (VG) and its *T-ΔH* diagram are presented. The VG is considered as countercurrent plate heat exchanger (PHE). It is worth mentioning that the evaporator section of the VG is divided into finite small elements in order to assume constant thermophysical properties of evaporating fluid for each element. The values of the parameters shown in figure 3 are provided in table 1.

Table 1. Parameters of ORC system.

Energy source			Organic Rankine cycle			Heat sink		
brine			organic fluid			cold water		
$\dot{V}_1$	[m^3h^{-1}]	10	$\dot{m}_2$	[kgs^{-1}]	*	$\dot{m}_3$	[kgs^{-1}]	*
t_{1w}	[°C]	105	t_{ev}	[°C]	53-68	t_{1c}	[°C]	10
t_{2w}	[°C]	60	t_{con}	[°C]	30	t_{2c}	[°C]	20
M	[kg/kg]	0.00-0.16	ΔT_p	[K]	*	-		
-			ΔT_{sup}	[K]	5			

Star sign '*' means that the quantity is a result of calculation.
Pinch point temperature ΔT_p varies in the interval: 7,5-16,5 K.

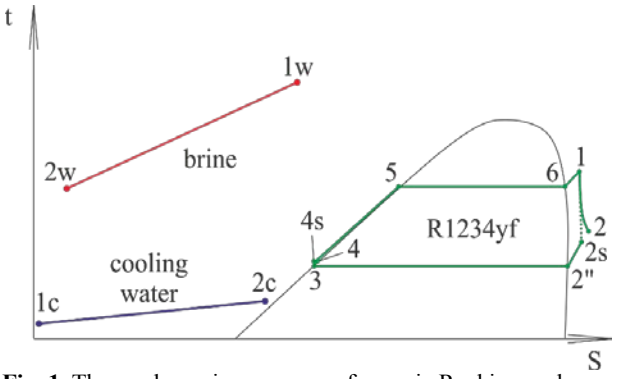

Fig. 1. Thermodynamic processes of organic Rankine cycle.

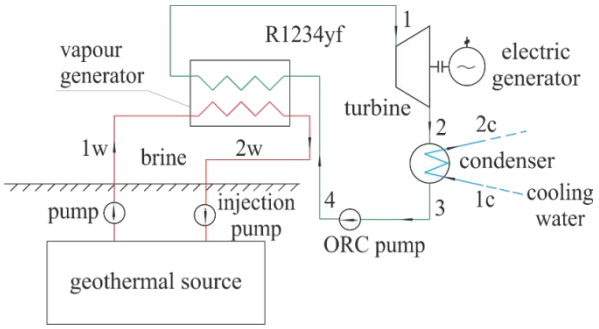

Fig. 2. ORC power plant.

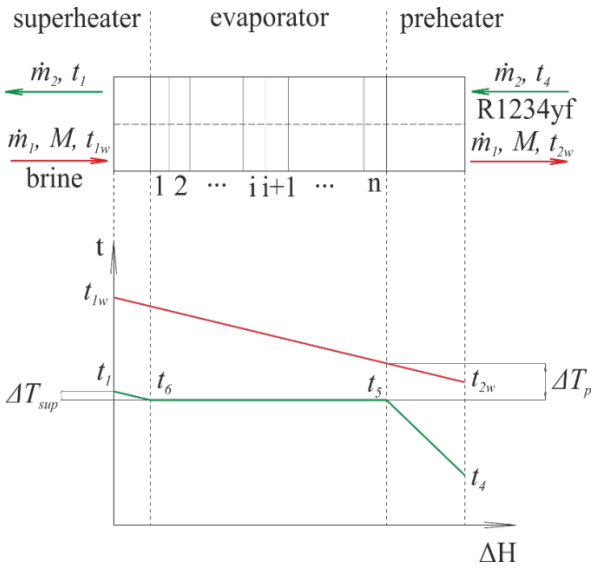

Fig. 3. Temperature field in a vapour generator.

2.2 Calculation model

The proposed model is created in order to reflect if there exists significant influence of the salination of the geothermal water on the optimum evaporation temperature of the working fluid in ORC power plant. However, it is difficult to make a comprehensive optimization using only single objective functions, since, during designing process of ORCs, it is impornant to include several factors, such as: thermodynamic, economic or environmental. In that model, multi-

objective optimization (MOO) approach has been proposed with multi-objective function *G(X)*, which consists of the quantities that are most substantially affected by decision variables, i.e.: the evaporation temperature t_{ev} and the mineralization M of the brine. Component quantities are the following: heat exchanger area of the vapour generator A_{VG}, net power output of ORC system N_{out}, overall exergy destruction rate δB_{tot} in the system and exergy drop ΔB_w of the geothermal water at the inlet and outlet .

Calculations have been made using *MATLAB 2017b* software [15] with *REFPROP 9.1* [16] as database of the thermophysical properties of R1234yf fluid.

2.2.1 Optimization model

The optimization model has been solved using weighted sum method with aforementioned *G(X)* as objective function, which, in this case, is the composition of two single objective functions:

$$G(X) = w_1 f_1^{\,n} + w_2 f_2^{\,n} \tag{1}$$

Single objective functions, which are to be minimised, can be written as follows:

$$f_1 = \frac{A_{VG}}{N_{out}} \tag{2}$$

$$f_2 = \frac{\delta B_{tot}}{\Delta B_w} \tag{3}$$

Function f_1 is an economic indicator, while function f_2 is called sustainability index *SI*, which determines the influence on the environment. However, in equation (1), normilized forms of the functions (2) and (3) have to be considered, as units and ranges of their values are different. In general, function f can be transformed to normalized form using the following formula:

$$f^n = \frac{f(x) - f_{\min}}{f_{\max} - f_{\min}} \tag{4}$$

where: f_{min} and f_{max} are minimum and maximum values of the objective function f in considered range of decision variable x. The intervals of decision variables, i.e. evaporation temperature t_{ev} and mineralization M of the brine are provided in table 1.

The assigned values of weights are the same: $w_1=w_2=0.5$, as both of the component objective functions f_1 and f_2 are considered to have the same level of significance.

2.2.2 Thermodynamic and heat transfer model

Heat transfer area of vapour generator A_{VG}

A_{VG} in this model is considered to be the sum of preheater, evaporator and superheater, which, using heat transfer formula, can be written in the following form:

$$A_{VG} = \frac{\dot{Q}_{pre}}{k_{pre}\Delta T_{\log pre}} + \sum_{i=1}^{n} \frac{\dot{Q}_i}{k_i \Delta T_{\log i}} + \frac{\dot{Q}_{\sup}}{k_{\sup}\Delta T_{\log \sup}} \tag{5}$$

It is worth to remind that the evaporator section (middle part of the (5) equation) is divided into finite small elements (see figure 3), so each quantity is determined with respect to i-th fininte element.

Heat fluxes for preheater, evaporator and superheater sections can be obtained from energy balance equation. On the assumption that ORC power plant is in steady state as well as there is no heat loss, corresponding heat fluxes can be calculated from the following formulas:

$$\dot{Q}_{pre} = \dot{m}_2 (h_5 - h_4) \tag{6}$$

$$\dot{Q}_i = \dot{m}_2 (h_{i+1} - h_i) \tag{7}$$

$$\dot{Q}_{\sup} = \dot{m}_2 (h_1 - h_6) \tag{8}$$

where enthalpies corresponding to states of working fluid (see figure 1 or 2) are determined using *Refprop* database. Enthalpy h_4 is obtained using equation (23). Mass flow rate of the R1234yf can be calculated from the following equation:

$$\dot{m}_2 = \frac{\dot{Q}_1}{q_{4-1}} = \frac{\rho_1 \dot{V}_1 c_{p1}(t_{1w} - t_{2w})}{h_1 - h_4} \tag{9}$$

As has been mentioned before, density ρ_1 and specific heat c_{p1} of the geothermal water should be considered as function of temperature as well as mineralization of the brine. Equations of these properties provided in [17] are as follows:

$$\begin{aligned}\rho_1(t,M) = {} & a_1 + a_2 t + a_3 t^2 + a_4 t^3 + a_5 t^4 + \\ & + b_1 M + b_2 M t + b_3 M t^2 + b_4 M t^3 + b_5 M^2 t\end{aligned} \tag{10}$$

where: a_1=9.999·10^2, a_2=2.034·10^{-2}, a_3=-6.162·10^{-3}, a_4=2.261·10^{-5}, a_5=-4.657·10^{-8}, b_1=8.020·10^2, b_2=-2.001, b_3=1.677·10^{-2}, b_4=-3.060·10^{-5}, b_5=-1.613·10^{-5} for the range of applicability: 0<t<180 °C, 0<M<0.16 kg·kg^{-1}

$$c_{p1}(T,M) = A + BT + CT^2 + DT^3 \tag{11}$$

where:

$$A = 5.328 - 9.760 \cdot 10^{-2} \cdot M + 4.040 \cdot 10^{-4} \cdot M^2$$

$$B = -6.913 \cdot 10^{-3} + 7.351 \cdot 10^{-4} \cdot M - 3.150 \cdot 10^{-6} \cdot M^2$$

$$C = 9.600 \cdot 10^{-6} - 1.927 \cdot 10^{-6} \cdot M + 8.230 \cdot 10^{-9} \cdot M^2$$

$$D = 2.500 \cdot 10^{-9} + 1.666 \cdot 10^{-9} \cdot M - 7.125 \cdot 10^{-12} \cdot M^2$$

for the following range of applicability: 273.15<T<453.15K, 0<M<180 g·kg^{-1}. It is mandatory to use units of temperature and mineralization such as in given ranges. Resulting density and specific heat are in kg·m^{-3} and kJ·kg^{-1}K^{-1} respectively.

The logarithmic mean temperature difference ΔT_{log} can be calculated using equation :

$$\Delta T_{\log} = \frac{t_1' - t_2'' - \left(t_1'' - t_2'\right)}{\ln \frac{t_1' - t_2''}{t_1'' - t_2'}} \tag{12}$$

where superscripts: ' and '' indicates inlet and outlet temperatures respectively.

Overall heat transfer coefficient k can be obtained from the general formula:

$$k = \left(\frac{1}{h_1} + \frac{\delta}{\lambda} + \frac{1}{h_2} \right)^{-1} \tag{13}$$

δ=0.6mm and λ=18Wm^{-1}K^{-1} are the assumed values of thickness and thermal conductivity of the heat exchanger plate respectively. Depending on which section of the vapour generator is being analysed, different correlations of Nusselt number Nu_2 for organic working fluid side are used. Definition of Nusselt number allows to calculate heat transfer coefficient h:

$$h = \frac{Nu\lambda_l}{d_h} \tag{14}$$

where d_h is calculated as double distance h_0 between plates (d_h=2·1.5=3mm).

In case of geothermal water side, the correlation for Nu_1 is the same for all sections and has the following form [18]:

$$N_1 = C\left(\mathrm{Re}_1^{\left(0.728+0.0543\sin\left(\frac{2\pi\beta}{90}\right)+3.7\right)} \right) \mathrm{Pr}_1^{1/3} \left(\frac{\mu_1}{\mu_{wa}} \right)^{0.14} \tag{15}$$

where:

$$C = 0.2668 - 0.006967\beta + 7.244 \cdot 10^{-5}\beta^2 \tag{16}$$

The so called chevron angle is assumed to be equal to: β=60°. The Reynolds number Re is defined as follows:

$$\mathrm{Re} = \frac{v d_h \rho}{\mu} \tag{17}$$

Superheater section

The following Nusselt number correlation [19] for organic working fluid side has been used:

$$Nu_{\mathrm{sup}} = 0.2946 \cdot \mathrm{Re}_{\mathrm{sup}}^{\ 0.7}\, \mathrm{Pr}_l^{1/3} \tag{18}$$

Evaporator section

Yan and Lin [20] proposed the following correlation for two-phase flow boiling process:

$$Nu_{ev} = 1.926\, \mathrm{Re}_{eq}\, Bo_{eq}^{\ 0.3}\, \mathrm{Re}_l^{\ -0.5}\, \mathrm{Pr}_l^{1/3} \tag{19}$$

where boiling number is defined as:

$$Bo = \frac{q}{Gr} \tag{20}$$

Detailed description of the equation is provided in aforementioned article.

Preheater section

In case of preheating process of the R1234yf, the same correlation (14) for Nusselt number was used as for water side.

Net power output N_{out}

The general formula for N_{out} is the following:

$$N_{out} = \dot{m}_2 \left[h_1 - h_2 - \left(h_4 - h_3 \right) \right] \tag{21}$$

where the enthalpies h_2 and h_4 are calculated using definitions of isentropic efficiencies (equations (22) and (23)), which assumed values for a turbine and a pump are equal to: η_{iT}=80% and η_{iP}=75%.

$$h_2 = h_1 - \eta_{iT}\left(h_1 - h_{2s} \right) \tag{22}$$

$$h_4 = h_3 + \frac{h_{4s} - h_3}{\eta_{iP}} \tag{23}$$

Overall exergy destruction rate δB_{tot}

The total exergy destruction in analysed ORC system can be presented as the sum:

$$\delta \dot{B}_{tot} = \delta \dot{B}_{VG} + \delta \dot{B}_{con} + \delta \dot{B}_T + \delta \dot{B}_P \tag{24}$$

The components of equation (24) correspond to all elements of ORC system are shown in figure 2 and are explained below.

Vapour generator

The exergy destruction in every component can be calculated using Gouy-Stodola equation, which in case of VG has the following form:

$$\delta \dot{B}_{VG} = T_r \sum \Delta \dot{S}_{VG} \tag{25}$$

where subscript r means reference state, which level is characterized by temperature T_r=298.15K and pressure p_r=101325Pa. The sum of the entropy fluxes can be found from the entropy balance equation:

$$\sum \Delta \dot{S}_{VG} = \dot{m}_1 \left(s_{2w} - s_{1w} \right) + \dot{m}_2 \left(s_1 - s_4 \right) \tag{26}$$

Condenser

Similarly to the vapour generator, the equations of the exergy destruction and the entropy balance for condenser are the following:

$$\delta \dot{B}_{con} = T_r \sum \Delta \dot{S}_{con} \tag{27}$$

$$\sum \Delta \dot{S}_{con} = \dot{m}_3 \left(s_{2c} - s_{1c} \right) + \dot{m}_2 \left(s_3 - s_2 \right) \tag{28}$$

Turbine

For the turbine, Gouy-Stodola equation has the following form:

$$\delta \dot{B}_T = T_r \sum \Delta \dot{S}_T \tag{29}$$

where:

$$\sum \Delta \dot{S}_T = \dot{m}_2 (s_2 - s_1) \tag{30}$$

Pump

Analogically, for the pump:

$$\delta \dot{B}_P = T_r \sum \Delta \dot{S}_P \tag{31}$$

$$\sum \Delta \dot{S}_P = \dot{m}_2 (s_4 - s_3) \tag{32}$$

Exergy drop ΔB_w of the geothermal water

Exergy drop of the brine between inlet and the outlet of vapour generator can be calculated from:

$$\Delta B_w = \dot{m}_1 (b_{1w} - b_{2w}) \tag{33}$$

Using the definition of exergy, b_{1w} and b_{2w} are calculated as:

$$b_{1w} = h_{1w} - h_r - T_r (s_{1w} - s_{r1}) \tag{34}$$

$$b_{2w} = h_{2w} - h_r - T_r (s_{2w} - s_{r1}) \tag{35}$$

3 Results and discussion

In figures 4-10 overall results of thermodynamic and optimization analysis are presented. As can be seen in figure 4, heat transfer area A_{VG} of the vapour generator increases with the increase of evaporation temperature, which is, mostly, due to the fact that with the increase of t_{ev}, heat flux $\dot{Q}_i$ (see equation (7)) of the working fluid R1234yf also increases, which clearly involves A_{VG} (see equation (5)). However, with the increase of salination of a brine, there can be seen the opposite dependence. This fact is mainly influenced by the variability of the geothermal water heat flux $\dot{Q}_1$, as it is the function of mineralization M. Decreasing values of the heat flux $\dot{Q}_1$ with increasing mineralization M stems from an influence of the M on the thermophysical properties of the brine, i.e.: density ρ_1 and specific heat c_{p1}. It turns out that the density ρ_1 is increasing while the specific heat c_{p1} is decreasing with the increase of mineralization M, however – the overall effect, which comes from the product of ρ_1 and c_{p1} (see equation (9)), leads to the decrease of $\dot{Q}_1$. Moreover, the changes in heat flux $\dot{Q}_1$ affect heat fluxes transfered in preaheater, evaporator and superheater (see equations (6),(7),(8)), since the enegy balance equation must be conserved, thus decreasing values of $\dot{Q}_1$ lead to the less values of A_{VG}.

Net power output N_{out}, as can be seen in figure 5, is increasing with the evaporation temperature, since the mass flow rate $\dot{m}_2$, which affects N_{out}, depends on previously discussed $\dot{Q}_1$ (see equations (9) and (21)). For an analogical reason, N_{out} is decreasing with the mineralization M, as higher values of M correspond to the lower values of $\dot{m}_2$.

Figure 6 presents the results for the first objective function f_1, i.e. ratio of heat transfer area of the vapour generator A_{VG} and net power output N_{out}.

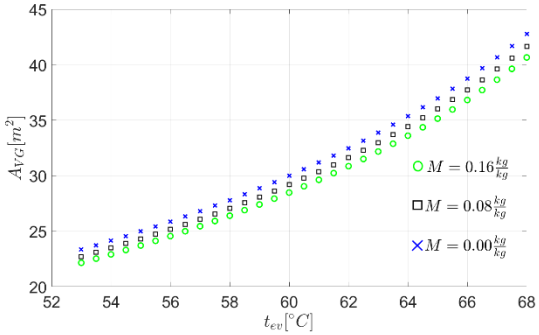

Fig. 4. Vapour generator area A_{VG} as the function of evaporation temperature t_{ev} for different levels ofmineralization M.

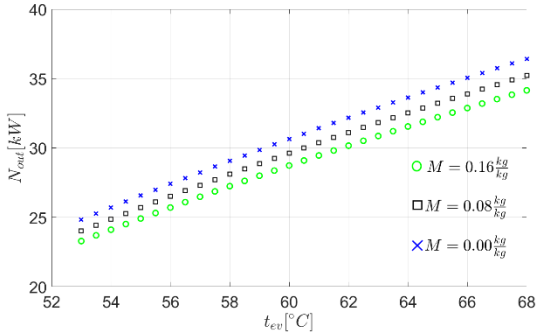

Fig. 5. Net power output N_{out} as the function of evaporation temperature t_{ev} for different levels of mineralization M.

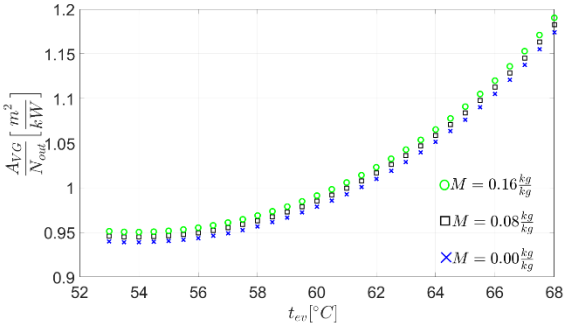

Fig. 6. The ratio of vapour generator area to the net power output as the function of evaporation temperature t_{ev} for different levels of mineralization M.

It is worth noticing that there exists optimum evaporation temperature of the function f_1 and it is located approximetaly at the temperature of 54°C. The influence of mineralization is relatively small, but negative – increasing values of M lead to increasing values of f_1 which is to be minimised.

Overall exergy destruction rate δB_{tot} is decreasing

with the increase of evaporation temperature, as can be seen in figure 7. It is worth mentioning that the greatest exergy destruction occurred in vapour generator. Moreover, these losses are changing most rapidly with respect to evaporation temperature t_{ev} and mineralization M. Therefore, it should come as no surprise that exergy destruction in the system is decreasing , as higher values of t_{ev} lead to smaller temperature differences between geothermal water and working fluid and therefore – to less entropy generation (see for instance equations (25) and (26)). The exergy destruction also decreases with respect to mineralization, which can be explained using equation (26). As has been mentioned before, mass flow rate of the working fluid $\dot{m}_2$ is decreasing with the increase of mineralization. Simultaneously, mass flow rate of the geothermal water $\dot{m}_1$ is increasing, because of the increase of the density ρ_1. The entropy drops of the water and working fluid are negative and positive respectively, thus the overall effect leads to the decrease of exergy destruction.

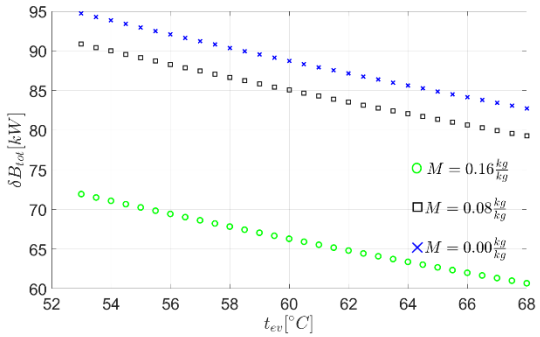

Fig. 7. Overall exergy destruction rate δB_{tot} as the function of evaporation temperature t_{ev} for different levels of mineralization M.

In figure 8, exergy drop of the geothermal water is changing with respect to only mineralization M, as quantities in equation (33) are independent on the evaporation temperature t_{ev} of the working fluid. The less values of ΔB_w for higher levels of mineralization can result from decreasing values of specific heat c_{p1}, which in turn affect the enthalpies that are the components in equations (34) and (35).

Figure 9 presents the results for the second objective function f_2, which is the ratio of total exergy destruction δB_{tot} to exergy drop of the geothermal water ΔB_w. This function is also known as sustainability index SI. Lower values of that indicator correspond to lower negative influence on an environment. The drop in of the values of the objective function with respect to evaporation temperature t_{ev} is obvious, since the exergy destruction from figure 7 has the same tendency and exergy drop of water from figure 8 is not changing. The mineralization M of the brine affect the objective function f_2 analogically as on its components. Although, that function does not indicate optimum evaporation temperature t_{ev} of working fluid, however, there can be seen that higer saturation temperatures would be more beneficial in this case.

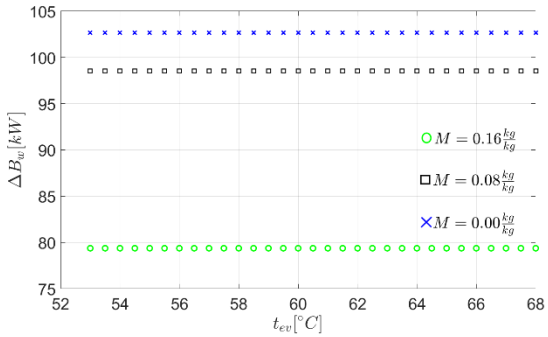

Fig. 8. Exergy drop ΔB_w of the geothermal water as the function of evaporation temperature t_{ev} for different levels of mineralization M.

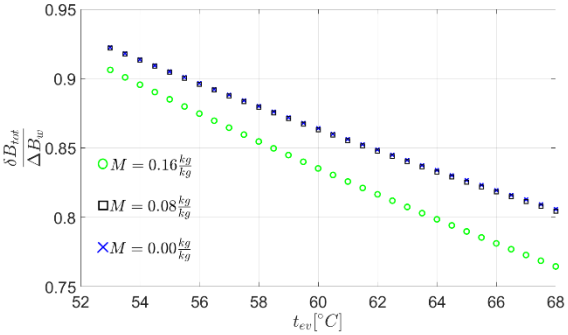

Fig. 9. Sustainability index SI as the function of evaporation temperature t_{ev} for different levels of mineralization M.

Finally, figure 10 presents the results for multi-objective function G. On the assumptions that have been made, i.e. equivalent importance (w_1=w_2=0.5) of both objective functions f_1 and f_2 and using evaporation temperature t_{ev} and mineralization M as decision variables, it turns out that optimum evaporation temperature equals to approximately 61°C, but more importantly, it is the same for all analysed levels of mineralization of the brine. This means that mineralization M has no influence on the choice of

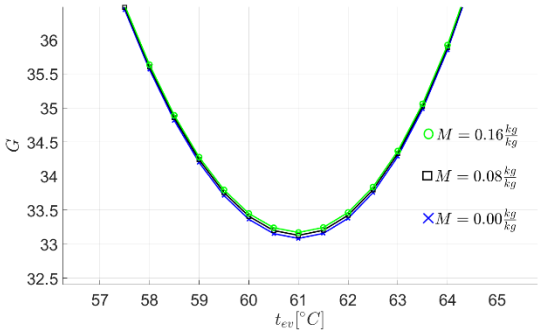

Fig. 10. Multi-objective function G as the function of evaporation temperature t_{ev} for different levels of mineralization M.

optimum evaporation temperature. Moreover, it can be seen that minimum values of the function G have been obtained for mineralization M=*0.00*. However, each of three curves almost coincide with each other, which

means that the overall influence of the mineralization *M* is almost negligible, which can be explained by the fact that single-objective functions f_1 and f_1 have presented the opposite relationship with respect to salination – f_1 was increasing and f_2 was decreasing for certain evaporation temperatures.

4 Conclusions

In the article, multi-objective function *G* has been created using performance indicators of ORC power plant, i.e. ratio of heat transfer area of vapour generator A_{VG} to net power output N_{out} (objective function f_1) and *SI* index (objective function f_2), which are to be minimised. The proposed calculation model allowed to conduct an analysis of the results from both: single- and multi-objective optimization perspective. The main aim of the paper was to resolve, if there is a significant influence of the mineralization on individual (f_1 and f_2) and global (*G*) ORC performance indicators as well as on the optimal evaporation temperature of the working fluid R1234yf. The presented results are important and can be used by scientists as well as by engineers, since they reflect, if there is a high risk of drop in economic (function f_1), environmental (function f_2) or overall (function *G*) index for different levels of mineralization *M*. The multi-objective problem has been solved using weighted sum method. The following conclusions were drawn:

- there is a low impact of the mineralization *M* of the brine on the single-objective functions f_1 and f_2, however in case of the first one the influence is negative (function f_1 takes higher values for higher levels of mineralization *M*), in the second one: positive (the values of f_2 are lower with respect to increasing levels of mineralization *M*),
- the multi-objective function *G* takes almost the same values for each of the analysed levels of mineralization *M* in considered interval of the evaporation temperature t_{ev}, which can result from the aforementioned opposite impacts of single-objective functions,
- the evaporation temperature t_{ev} corresponding to minimum value of *G* is the same (t_{ev}=61°C) for each of the mineralization *M* levels, i.e. for the adopted criteria, there is no influence of such parameter on the optimum evaporation temperature of R1234yf in considered ORC system.

Nomenclature

A – heat exchanger area [m^2]
Bo – boiling number
$\dot{B}$ – exergy flux [kW]
b_0 – width of plate [m]
c_p – specific heat capacity [J kg^{-1} K^{-1}]
d – diameter [m]
f – single-objective function
h – heat transfer coefficient [W m^{-2} K^{-1}] or specific enthalpy [Jkg^{-1}]
h_0 – pitch between plates [m]
G – density mass flux [kg s^{-1} m^{-2}] or multi-objective function
k – overall heat transfer coefficient [W m^{-2} K^{-1}]
L – length [m]
M – mineralization [kg kg^{-1}]
N_{out} – net power output [kW]
Nu – Nusselt number
$\dot{m}$ – mass flow rate [kg s^{-1}]
p – pressure [Pa]
q – density heat flux [W m^{-2}]
Re – Reynolds number
r – latent heat of vaporization [J kg^{-1}]
Pr – Prandtl number
S – entropy [kJ K^{-1}]
s – specific entropy [kJ kg^{-1} K^{-1}]
t – temperature [°C]
V – volume flowrate [m^3s^{-1}]
v – velocity [m s^{-1}]
w – weight

Greek symbols

β – chevron angle [°]
$\Delta\dot{B}_w$ – exergy drop of geothermal water [kW]
ΔH – enthalpy difference [kW]
ΔT – temperature difference [K]
δ – plate thickness [m]
$\delta\dot{B}$ – exergy destruction rate [kW]
η – efficiency
λ – thermal conductivity [W m^{-1} K^{-1}]
μ – dynamic viscosity [Pa s]
ρ – density [kg m^{-3}]

Sub- or superscripts

‘ – correspond to inlet
“ – correspond to outlet
1 – correspond to brine
2 – correspond to working fluid
3 – correspond to cooling water
c or con – condenser
ev – evaporation
h – hydraulic
i – correspond to section or isentropic
l – liquid
log – logarithmic
n – normalized
P – pump
p – pinch point
pre – preheater
r – reference state
VG – vapour generator
sup – superheater
T – turbine
w – water
wa – wall

References

1. I.H. Aljundi, *Effect of dry hydrocarbons and critical point temperature on the efficiencies of organic Rankine cycle*, Renew. En. **36** (2011)

2. A.A. Lakew, O. Bolland, *Working fluids for low-temperature heat source*, App. Ther. Eng. **30** (2010)
3. Z. Shengjun, W. Huaixin, G. Tao, *Performance comparison and parametric optimization of subcritical Organic Rankine Cycle (ORC) and transcritical power cycle system for low-temperature geothermal power generation*, App. En. **88** (2011)
4. J.P. Roy, M.K. Mishra, A. Misra, *Performance analysis of an Organic Rankine Cycle with superheating under different heat source temperature conditions*, App. En. **88** (2011)
5. J. Guo, M. Xu, L. Cheng, *Thermodynamic analysis of waste heat power generation system*, En. **35** (2010)
6. Bendig M., Favrat D., Marechal F., *Methodology for Identification of Suitable ORC-Cycle and Working-Fluid using Integration with Multiple Objectives*, Chem. Eng. Trans. **39** (2014)
7. J. Wang, Z. Yan, M. Wang, M. Li, Y. Dai, *Multi-objective optimization of an organic Rankine cycle (ORC) for low grade waste heat recovery using evolutionary algorithm*, En. Conv. and Man. **71** (2013)
8. L. Xiao, S.-Y. Wu, T.-T. Yi, C. Liu, Y.-R. Li, *Multi-objective optimization of evaporation and condensation temperatures for subcritical organic Rankine cycle*, En. **83** (2015)
9. A. Toffolo, A. Lazzaretto, G. Manente, M. Paci, *A multi-criteria approach for the optimal selection of working fluid and design parameters in Organic Rankine Cycle systems*, App. En. **121** (2014)
10. T.R. Marler, J.S. Arora, *The weighted sum method for multi-objective optimization: new insights*, Struct. Multidisc. Optim. **41** (2010)
11. H. Chen, Y.D. Goswami, E.K. Stefanakos, *A review of thermodynamic cycles and working fluids for the conversion of low-grade heat*, Renew. and Sustain. En. Rev. **14** (2010)
12. J. Bao, L. Zhao, *A review of working fluid and expander selections for organic Rankine cycle*, Renew. and Sustain. En. Rev. **24** (2013)
13. A.I. Papadopoulos, M. Stijepovic, P. Linke, *On the systematic design and selection of optimal working fluids for Organic Rankine Cycles*, App. Ther. Eng. **30** (2010)
14. M.T. Nasir, K.C. Kim, *Working fluid selection and parametric optimization of an Organic Rankine Cycle coupled Vapor Compression Cycle (ORC-VCC) for air condidioning using low grade heat*, En. and Build., **129** (2016)
15. The MathWorks Inc, MATLAB version R2017b. 2017.
16. E.W. Lemmon, M.L. Huber, M.O. McLinden, *Reference thermodynamic and transport properties – Refprop NIST standard reference base 23,* Version 9.1
17. M. Miecznik, *Error in the estimation of the potential for electricity generation in a binary ORC systems associated with variation of thermodynamic parameters of geothermal water*, Geotermia, Zrównoważony Rozwój nr 2/2013
18. J.T. Cieśliński, A. Fiuk, K. Typiński, B. Siemieńczuk, *Heat transfer in plate heat exchanger channels: Experimental validation of selected correlation equations*, Archives of Thermod. **37** (2016)
19. Z. Janković, J. Sieres, F. Cerdeira, B. Pavković, *Analysis of the impact of different operating conditions on the performance of a reversible heat pump with domestic hot water production*, Inter. Journ. of Refri. **86** (2018)
20. Y.Y. Yan, T.F. Lin, *Evaporation heat transfer and pressure drop of refrigerant R134a in a plate heat exchanger*, ASME J. Heat Transfer. **121 (**1999)